J Therm Spray Tech (2017) 26:1888–1897
https://doi.org/10.1007/s11666-017-0643-5

PEER REVIEWED

Mechanical Performance of Cold-Sprayed A357 Aluminum Alloy Coatings for Repair and Additive Manufacturing

K. Petráčková[1] · J. Kondás[2] · M. Guagliano[1]

Submitted: 9 May 2017 / in revised form: 11 September 2017 / Published online: 25 September 2017

Abstract Cold-sprayed coatings made of A357 aluminum alloy, a casting alloy widely used in aerospace, underwent set of standard tests as well as newly developed fatigue test to gain an information about potential of cold spray for repair and additive manufacturing of loaded parts. With optimal spray parameters, coating deposition on substrate with smooth surface resulted in relatively good bonding, which can be further improved by application of grit blasting on substrate's surface. However, no enhancement of adhesion was obtained for shot-peened surface. Process temperature, which was set either to 450 or 550 °C, was shown to have an effect on adhesion and cohesion strength, but it does not influence residual stress in the coating. To assess cold spray perspectives for additive manufacturing, flat tensile specimens were machined from coating and tested in as-sprayed and heat-treated (solution treatment and aging) condition. Tensile properties of the coating after the treatment correspond to properties of the cast A357-T61 aluminum alloy. Finally, fatigue specimen was proposed to test overall performance of the coating and coating's fatigue limit is compared to the results obtained on cast A357-T61 aluminum alloy.

✉ K. Petráčková
klara.petrackova@gmail.com; Klara.Petrackova@polimi.it

J. Kondás
jan.kondas@impact-innovations.com

M. Guagliano
Mario.Guagliano@polimi.it

[1] Department of Mechanical Engineering, Politecnico di Milano, Via G. La Masa, 1, 20156 Milan, Italy

[2] Impact Innovations GmbH, Bürgermeister-Steinberger-Ring 1, 84431 Haun, Rattenkirchen, Germany

Keywords A357 aluminum alloy · cold spray · fatigue limit · heat treatment · mechanical properties

Introduction

Aeronautical sector is likely to experience significant growth in the next few years, especially in the Asia Pacific and the Middle-East regions (Ref 1, 2). Therefore, an increasing attention is directed toward reliable maintenance services and improved repair strategies to extend aircraft's lifetime as well as repair of castings with manufacturing defects. The improvement of existing repair methods and development of new solutions would allow for cost and pollution reduction resulting from avoidance of damaged component's substitution and decrease of high-energy consumption of current technologies as well as use of toxic gases (Ref 2). Lastly, additive manufacturing of components is growing in importance in both aeronautical and automotive fields.

Cold spray, a member of the family of thermal spraying, provides a promising solution to aforementioned issues. As an "environmentally friendly' technology, it holds an advantage over other methods (welding, plasma spray etc.). Its main feature is solid-state nature of particles deposition due to the very low process gas temperatures employed. The particles are accelerated to supersonic velocities by compressed gas in converging–diverging nozzle. Upon impact, high kinetic energy of the particle generates adiabatic shear instability, which is considered to be responsible for successful bonding between particle and substrate or already deposited coating. Bonding can be also created by mechanical interlocking, when impacting particles anchor to rough substrate's surface. However, bonding only occurs if particle velocity exceeds critical velocity,

Table 1 Chemical analysis of A357 aluminum alloy

Si	Cu	Mg	Mn	Fe	Zn	Ti	Be	Total (Cr, Ga, Ni, Pb, Sn)
6.7	0.004	0.4	0.001	0.09	0.01	0.07	0.0001	0.12

which is a threshold value depending on spray process parameters, material, and particle size and morphology (Ref 3-5). Good ductility makes aluminum and aluminum alloys convenient material for cold spray applications, and, in general, successful bonding is generated via plastic deformation upon particle impact (Ref 6, 7).

Among the alloys used for manufacturing aeronautic parts, A357 aluminum alloy is one of the most widely used, due to its excellent casting properties with good weldability. When heat treated, ultimate tensile strength exceeds 310 MPa, ductility is well above 3% depending on the treatment applied (Ref 8), and the alloy possesses a very good corrosion resistance (Ref 9, 10). Thanks to high strength-to-weight ratio, the alloy finds applications mainly in automotive and aerospace industry. In aeronautical industry, A357 aluminum alloy is used to produce lightweight, high-strength, complex castings, i.e., aircraft and missile components like brackets, frames, motion transfer and gearbox housings.

This study was performed in the framework of CORSAIR (Ref 2), a research program funded by the European Union. It is aimed at investigating and characterizing mechanical behavior of A357 coating produced by cold spray. There are no journal publications pertaining to cold-sprayed A357 aluminum alloy. Even though some repairs of A357 components have been documented, 4047 or 6061 alloys were always used as powder feedstock (Ref 11). Cold spray deposition of wide range of aluminum alloys has been studied under both high and low pressure. In this study, current technological limits of the process are shifted forward by using a high-pressure system with water-cooled SiC nozzle that allows nitrogen process gas to reach temperatures higher than the state of the art, and thus high impact velocity, a critical factor for establishing strong bonding (Ref 12, 13). The coating was deposited on the same material substrate, as one of the aims is to characterize mechanical performance of the coating and develop procedure to restore components with damage (pit, scratch, cracks…) using the same material as the repaired component. Set of experiments was carried out to determine mechanical properties such as adhesion, cohesion, presence of residual stresses in the coating, ductility after heat treatment and fatigue strength.

Bond strength is related to the surface finishing of the substrate, and it is known that increasing surface roughness (by grit blasting or shot peening) may improve adhesion significantly (Ref 14, 15). In addition, some rotating bending test results have shown that shot peening prior coating deposition improves fatigue strength (Ref 16, 17) due to compressive residual stresses induced by that treatment. In the present study, different surface preparations are used to determine its influence on bond strength of A357 coating.

Apart from cohesion strength of the coating, tensile test of heat-treated coatings was performed to address a typical cold spray coatings' feature—zero ductility. Significant increase in ductility was observed after heat treatment (HT) (Ref 18, 19). An alternative solution treatment of A357 freestanding coating is applied (Ref 20), and its effect on the tensile properties of the coating is analyzed.

Finally, a fatigue test is proposed to assess overall performance of the coating and potential of cold spray technology to successfully repair loaded parts. If the coating retains strength of the original material, a great step in structural repairs is accomplished extending possible cold spray applications.

Materials and Methods

Powder and Process Parameters

Commercially available inert gas atomized A357 aluminum alloy powder, with particle size distribution of 15-63 μm, supplied by Valimet Inc. (US), was used for this study. Table 1 reports chemical analysis of the powder. SEM images show spherical particles with satellites of sizes ranging between 15 and 63 μm in diameter (Fig. 1). A357 coatings were deposited with Impact Spray System 5/8 (60 bar upgrade, Impact Innovations GmbH, Germany). Preliminary trials were carried out with varying gas temperature (200-550 °C), pressure (20-57 bar), spray angle (60°-90°), and stand of distance (10-50 mm). Only one parameter was varied at the time, and porosity of the coating and deposition efficiency were evaluated for each sample. Porosity measurement was taken by image analysis of coating's cross-sectional images using the Keyence VHX-5000 digital microscope, and deposition efficiency was measured relatively, comparing thickness of the coatings, which was built with identical number of passes of the spray nozzle for each sample. Final spray parameters, shown in Table 2, were chosen based on lowest porosity and highest deposition efficiency evaluated. Almost identical results in terms of porosity were obtained for coatings sprayed at 450 and 550 °C process gas temperature. It is to be noted that nozzle experiences clogging after spraying for certain time at 550 °C. Despite its current

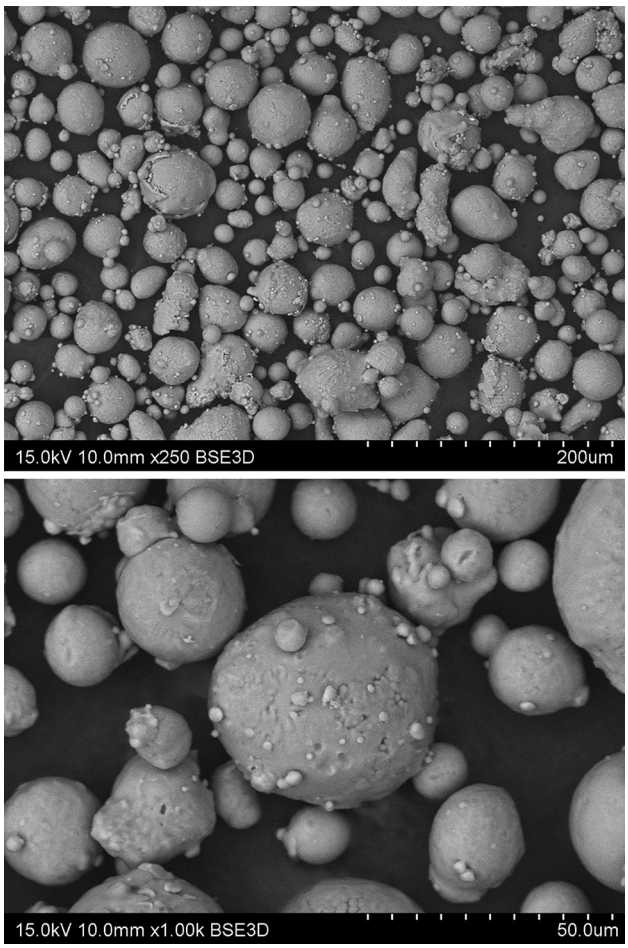

Fig. 1 BSE images of powder feedstock

Table 2 Spray process parameters

Temperature	450 °C or 550 °C
Pressure	57 bar
Spray angle	90°
Gun travel speed	500 mm/s
Stand-off distance	15 mm
Gas	Nitrogen

technical limitation, 550 °C propelling temperature was selected to produce coatings for mechanical testing, too. This follows current trends in cold spray technology for dimensional restoration, which head toward increasing the process parameters, thus particle velocity, to enhance coating properties deposited using nitrogen as propelling gas (Ref 12). Coatings deposited at 550 °C were tested only for adhesion, cohesion and residual stress measurement. The last two tests published here, tensile test of freestanding coatings and fatigue test, were only performed on coatings produced at 450 °C.

Table 3 Surface roughness

	AM	GB	SP	SP-SR
R_a, μm	1.02 ± 0.05	7.54 ± 0.6	2.40 ± 0.29	2.40 ± 0.29

Adhesion Tests

Bond strength test was performed according to standard procedure (Ref 21) using MTS tensile test machine. Coating with thickness of 0.8 mm was deposited on 5-mm-thick disks of 25.4 mm in diameter and glued to the fixtures by FM 1000 adhesive (Cytec Engineered Materials). Performance of the glue was verified on three specimens, which failed at 69.4 ± 1.8 MPa corresponding to the producer specifications. Five sets, each containing three samples, were tested in total. For the first set, coating was deposited at 550 °C onto grit-blasted surface. Only one set was produced at this temperature due to aforementioned nozzle clogging. Other four sets were sprayed at 450 °C, but following different surface preparations were applied prior spraying. At first, no surface treatment was used leaving disks as machined with fine surface finish (abbrev. AM). Second, two sets of disks underwent shot peening (SP) using ceramic shots Z300 (size of 0.3-0.425 mm) (Ref 22), intensity of 10.9 A and 100% coverage (detail description of mentioned parameters can be found in Ref 23). One of the shot-peened sets (SP-SR) was subsequently stress relieved (30 min at 150 °C) (Ref 24) to determine any influence of residual stresses on coating adhesion. Last treatment used was grit blasting (GB) performed with Al_2O_3 particles (63-90 μm) with process gas pressure of 30 bar using the same cold spray device. Resulting average surface roughness of the substrate is listed for each treatment in Table 3. It is to be noted that latter GB set was originally composed of three samples; however, non-uniform results required additional tests to be performed counting six sprayed coupons in total.

TCT Tests

Cohesion strength of the coating was measured on set of three specimens for each condition by means of tubular coating tensile (TCT) test as proposed in Ref 25. Coating thickness of 1 mm was deposited on two cylinders (diameter of 24 mm) connected by a screw. The coating was built with 28 passes (with gun travel speed of 5 mm/s and substrate rotation of 380 rpm). MTS tensile test machine with self-aligning adapters was used to perform the test. The specimen's configuration induces a stress concentration in the coating during the test. This is taken in account by multiplying the measured strength by a factor of 1.5 (Ref 25).

Residual Stress Measurement

Residual stresses in the coating were measured by AST X-Stress 3000 x-ray diffractometer. Coating was deposited on the same disks as those used for adhesion tests and correspond to AM condition. Measurement was taken on area of 2 mm of diameter in the middle of the disk with use of Cr tube radiation (diffraction angle equals to 139°, $\sin^2\psi$ method). Coating was removed toward substrate in steps by electropolishing (94% acetic acid and 6% perchloric acid solution). 0.2-0.25 mm of coating was removed in each step.

Tensile Test of Freestanding Coating

Four flat tensile specimens were machined from coated plates shown in Fig. 2. Two of the specimens underwent heat treatment. Although casting standards often do not allow for solution heat treatment of machined components (as it is the case of repair application) due to possible deformations induced at such high temperatures, it is of interest to apply heat treatment procedure according to Table 4 (Ref 20). This treatment can be used for components without specific requirement for HT like prototypes or additive manufactured parts. The results are compared to mechanical properties obtained on cast A357-T61. T61 is treatment applied to forgings, and it is similar to the proposed alternative HT used for coatings. The other two freestanding coating specimens were tested as sprayed to serve as a reference and, in addition, as a verification of correction factor used in TCT test evaluation. All the tests were carried out on MTS machine at room temperature according to Ref 26. Specimen's dimensions are displayed in Fig. 3. It is to be noted that thickness of the specimens is given by the thickness of the sprayed coating. Unfortunately, some problems occurred while machining, thus as-sprayed specimens have different thickness (b_0) as it is listed in Table 6 in the results section.

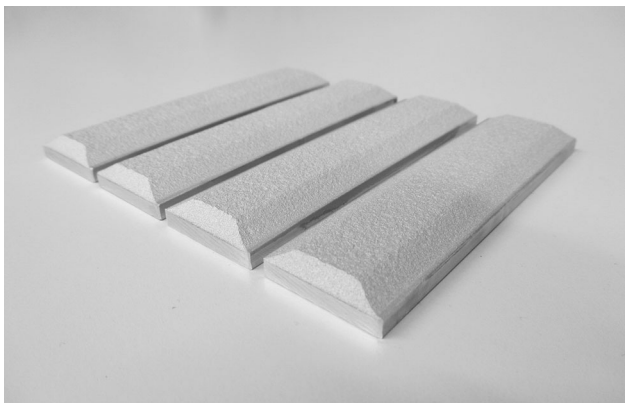

Fig. 2 Coating before machining

Table 4 HT steps (Ref 19)

Step	Parameter	Value
Solution treatment	Temperature	543 °C ± 5 °C
	Holding time	8.50 h
Quench	Temperature	Water quenching max. 32 °C
	Holding time	···
Artificial aging	Temperature	160 °C ± 5 °C
	Holding time	6.75 h

Fatigue Testing

Two sets, each composed of eleven specimens, were tested under cyclic loading. First set was machined from cast A357-T61 and served as a reference for bulk performance. The geometry of the specimen is displayed in Fig. 4. Another set of specimens was produced in two steps. In the first step, substrate material was machined (from the same cast bar) with distinct reduction of cross section in the central part of the specimen as it is shown in Fig. 5 (top). The specimen was produced from the same cast bar as the first set of specimens with all remaining dimensions corresponding to Fig. 4. In the second step, the coating was deposited on the reduced section, which was grit-blasted prior spraying (not shown in Fig. 5) leaving surface with $R_a = 7.5 \pm 0.6$ µm. The coating was built with 30 passes (with gun travel speed of 5 mm/s and substrate rotation of 382 rpm). Excess of coating (bottom specimen in Fig. 5) was removed by conventional machining (1500 rpm, tool travel speed 0.04 mm/rotation) to match dimensions displayed in Fig. 4. Red rectangle (Fig. 4) denotes portion of the specimen with the coating, which reaches maximum thickness of 1.5 mm in the middle of the specimen. Before testing, eleven coated specimens were polished with

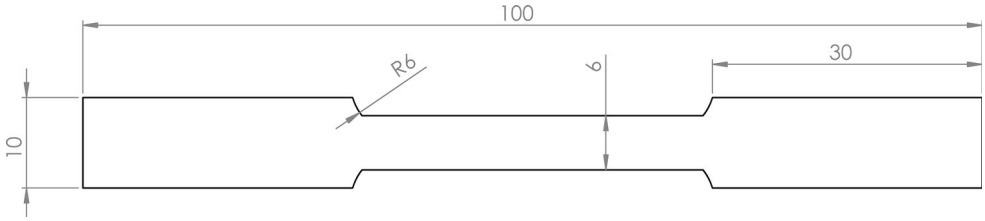

Fig. 3 Dimensions of the flat tensile specimen in mm (thickness of each specimen is listed in Table 6 as b_0)

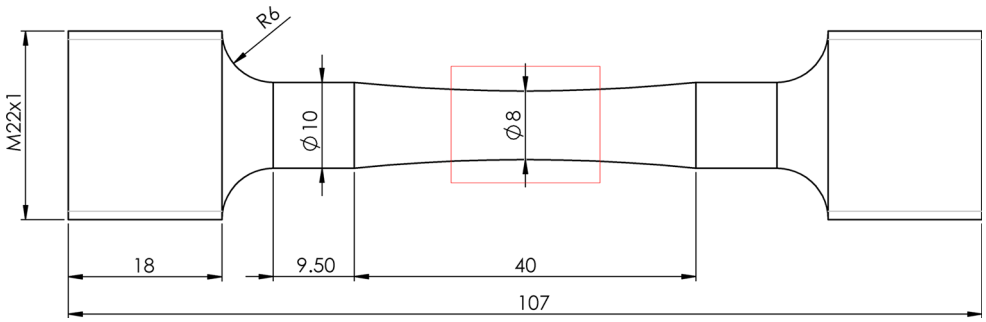

Fig. 4 Dimensions of fatigue specimens in mm

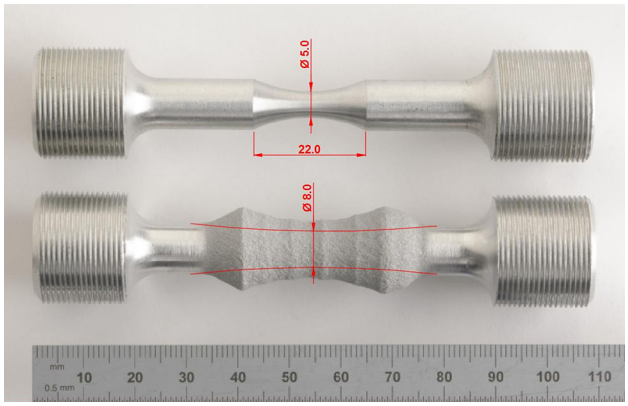

Fig. 5 Fatigue specimen: base material before (top) and after (bottom) coating deposition

grinding paper and three were left as machined to determine influence of surface finishing on fatigue properties. Room temperature axial fatigue tests were performed using high-frequency test machine Rumul Testronic ($R = -1$, $f = 120$ Hz), and 5 million cycles was considered as run-out. Stair-case method (Ref 27) was used to evaluate fatigue limit in both cases. Zeiss EVO50 scanning electron microscopy and Leitz Aristomet optical microscope were used to observe fractured surface and coating substrate interface.

Results and Discussion

Adhesion Strength

Results of all the tests are listed in Table 5 together with tested conditions and type of failure. Comparison of the two shot-peened sets (SP and SP-SR) aims to be qualitative; hence, no measurements of residual stresses in the substrate were taken. However, surface roughening is evidence of cold working resulting in compressive residual stresses in the substrate. These compressive stresses are relaxed by heat treatment (SP-SR). Considering this, the comparison shows that residual stresses in the substrate have no influence on adhesion, as the average strength for both conditions is approximately 45 MPa. When compared with as machined set (AM), it can be concluded that surface state induced by shot peening is not able to improve bond strength. Adhesion strength of 45 MPa was measured for coatings deposited on smooth surface (AM). This might suggest that metallurgical boding occurred in some portion of the interface (Ref 28). Significant adhesion improvement was achieved, when grit blasting was employed. In this way, bond strength of the coating exceeds the strength of the glue. This is completely valid for the results obtained for 550 °C process temperature as all the specimens experienced uniform failure in the glue layer. In case of the 450 °C, one specimen failed with mixed interfacial-cohesion failure at 62.2 MPa and very local interface failure was observed on other two specimens. The local interface failure (glue accounts for most of the fracture area) is likely to cause weak results of 54.8 ± 2.6 MPa. Three remaining samples fractured in glue at 68.8 ± 4.2 MPa, which is the value displayed in Table 5. The non-uniform failures suggest that actual bond strength was reached considering some results dispersion. This shows that adhesion strength increases when process temperature rises from 450 to 550 °C, which is in agreement with observations that higher impact velocity creates better bonding (Ref 12, 29). In both cases, increase in bond strength can be attributed to surface roughness introduced by grit blasting, which promotes mechanical interlocking, and possibly metallurgical bonding by breaking oxide films on surface and thus cleaning the surface (Ref 28).

Cohesion Strength

The cohesion strength was evaluated through TCT tests, and the following results were obtained by multiplying measured stress by factor of 1.5. The average coating strength is 214 ± 7.8 MPa, resp. 358 ± 47 MPa, in case of 450 °C process temperature used, resp. 550 °C. Clearly, cohesion strength rises with increase in spraying temperature, which conforms to already published findings (Ref 12). It is to be noted that the wide scatter in the second case (550 °C) results from non-uniform failure of one of the

Table 5 Adhesion test results (see 2.2 for the designation)

Surface preparation	AM	SP	SP-SR	GB	GB
Temperature, °C	450	450	450	450	550
Surface roughness R_a, µm	1.02 ± 0.05	2.40 ± 0.29	2.40 ± 0.29	7.54 ± 0.60	7.54 ± 0.60
Bond strength, MPa	45.2 ± 2.0	44.7 ± 4.1	44.5 ± 5.5	68.8 ± 4.2	70.2 ± 3.2
Fracture	Interface	Interface	Interface	Glue/mixed	Glue

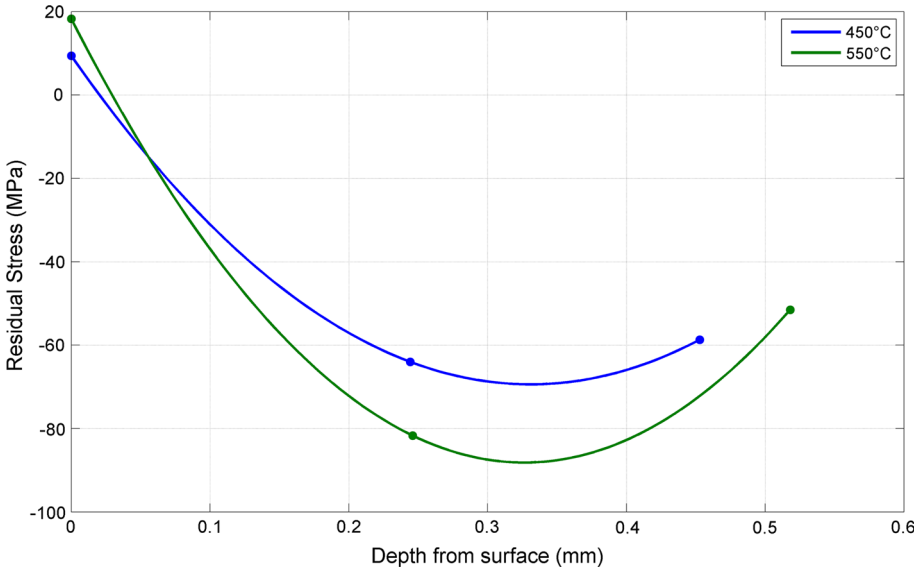

Fig. 6 Principal stress I

three specimens. A small delamination from the substrate cylinders was observed.

Residual Stresses

During cold spraying, it is in generally assumed that compressive residual stresses prevail in both coating and substrate due to the peening action during the impact of the powder against the substrate (Ref 30, 31). Figure 6 and 7 shows results in terms of in-plane principal stresses evaluated in different depth points through coating. However, only coating surface and other two measurements in coating depth are valid as upon approaching interface, it was not possible to detect any x-ray intensity peaks and thus no results were obtained. No values were detected in the substrate close to the interface either. The most likely explanation is that crystal lattice is highly distorted due to the high-speed impacts of particles similar to Ref 32, 33. Both samples, processed at different spraying temperature, yield comparable results, exhibiting zero or small tensile residual stress on the surface while compressive residual stresses are detected below coating surface. The difference between both curves is negligible as the measured stresses are overall quite low. Interestingly, increase in temperature does not influence residual stresses in the coating. This implies that temperature of particles sprayed under both conditions (450 and 550 °C gas temperature) approaches annealing temperature of A357 aluminum alloy, which is 540 °C (Ref 34), and in this way, peening effect is reduced (Ref 35). Thanks to short exposure to the carries gas, particle does not have time to reach such high temperature during its flight. However, a significant increase in temperature occurs after the impact, when high kinetic energy of the particle, resulting also from high process pressure (57 bar) used, is converted into heat responsible for stress relieving process acting at the expense of peening process. As a conclusion, coatings sprayed at both temperatures will yield nearly same residual stress profile, which is equibiaxial and mostly in compressive stress state.

Tensile Properties of Bulk Coating

Table 6 displays complete results obtained from tensile tests including specimens' dimensions needed to evaluate mechanical properties (D_0 is diameter of specimen, a_0 is width of the specimen, l_0 is gauge length, and b_0 is thickness of the specimen). As-sprayed specimens show typical brittle behavior, while cold-sprayed specimens after HT demonstrate increase in both strength and ductility. Ultimate tensile strength of heat-treated coating almost doubles with respect to the as-sprayed specimens and reaches bulk material performance. Ductility exceeds 5%,

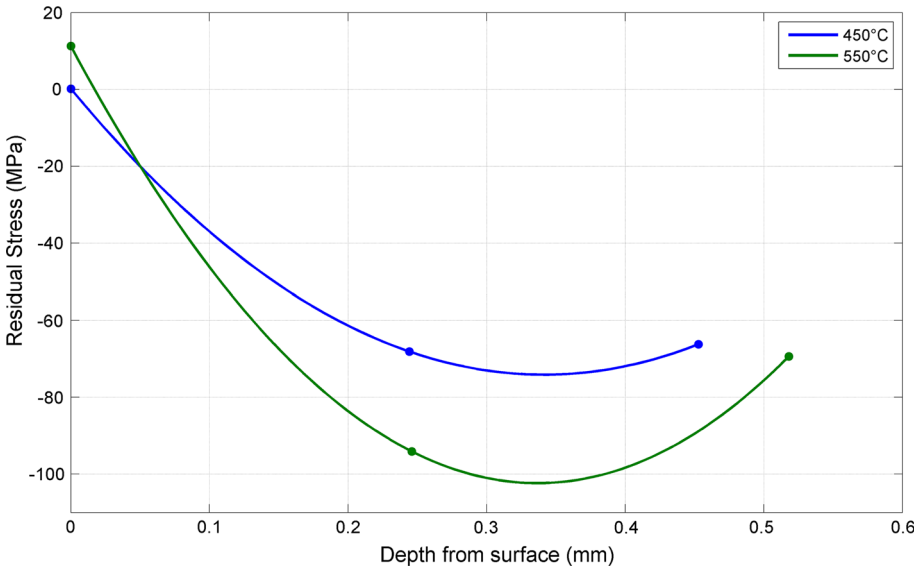

Fig. 7 Principal stress II

Table 6 Tensile test results

Specimen	D_0, mm	a_0, mm	b_0, mm	l_0, mm	E, GPa	$R_{p0,2}$, MPa	R_m, MPa	A_5, %
CS AS 1	···	6	1.9	25	62	···	145	···
CS AS 2	···	6	2.2	25	63	···	172	···
CS HT 1	···	6	2.9	25	68	201	298	5.8
CS HT 2	···	6	2.9	25	69	208	300	5.4
Cast 1	6.1	···	···	25	72	152	305	4.8
Cast 2	6.1	···	···	25	72	210	310	4.2

CS cold sprayed, *AS* as sprayed, *HT* heat treated

which is higher than ductility of bulk A357-T61 (abbrev. Cast 1 and Cast 2).

Before comparing cohesion strength obtained from TCT to the one measured on flat tensile test, it is to be noted that rupture occurred at radius part of the flat tensile specimen. The ultimate tensile stress determined from the test needs to be multiplied by a stress concentration factor. Finite element software ABAQUS was used to create a model of tensile specimen to determine the stress concentration coefficient. By comparing stress at the radius and stress in the constant cross-sectional part, the coefficient was found to be equal 1.26. The stress concentration factor was applied to the results from tensile test and compared to the cohesion strength (second line of Table 7). Two results are not enough to make any relevant conclusion about the correction factor for evaluation of the TCT test. Our results show that the value lies between 1.3 and 1.5.

Table 7 Comparison of cohesion strength determined from TCT and tensile test (process temperature of 450 °C)

UTS, MPa	TCT average	CS AS 1	CS AS 2
No correction	143 ± 8	145	172
After correction	214 ± 8	183	217

Fatigue Properties and Fractography

Coating cannot achieve the same performance as bulk material because it accounts for interface and porosity resulting from the nature of deposition process. In the same time, it needs to retain certain high percentage of its original fatigue strength for the repaired parts to continue the service. Table 8 shows fatigue limit calculated for both sets of specimens. Fatigue strength evaluated for coated specimens yields 94% of the strength determined for base material specimens indicating excellent fatigue performance of the coating. The second line in Table 8 shows surface roughness of the specimens tested. It is known that surface finish influences fatigue results. While arithmetic average of all measurements (R_a) is nearly the same for both sets of the specimens, the average distance between the lowest valleys and highest peaks (R_z) differs indicating slightly worse surface finish of base material specimens. This means that the results might be

Table 8 Comparison of fatigue limit obtained on base material and coated specimens

	Base material	Coating
Fatigue limit, MPa	105 ± 8.52	98 ± 4.23
Surface roughness R_a, μm	0.33 ± 0.06	0.35 ± 0.05
Surface roughness R_z, μm	3.61 ± 1.70	2.15 ± 0.10

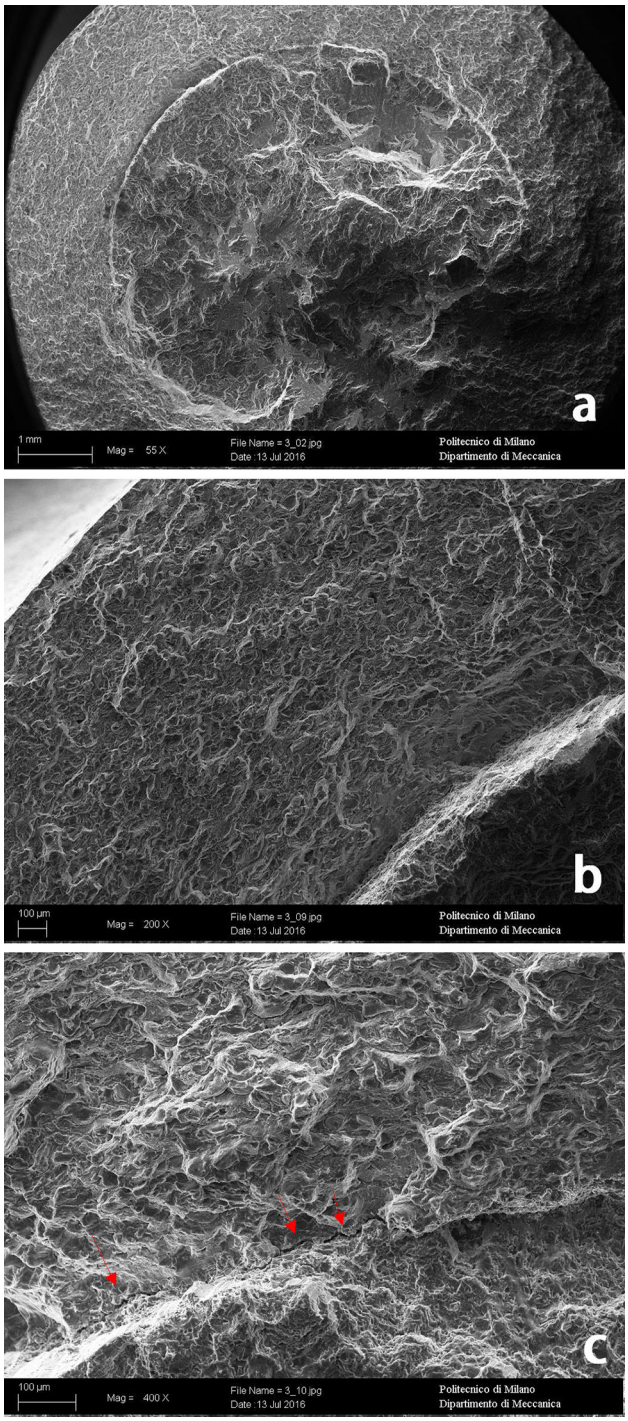

Fig. 8 SEM images of fractured surface

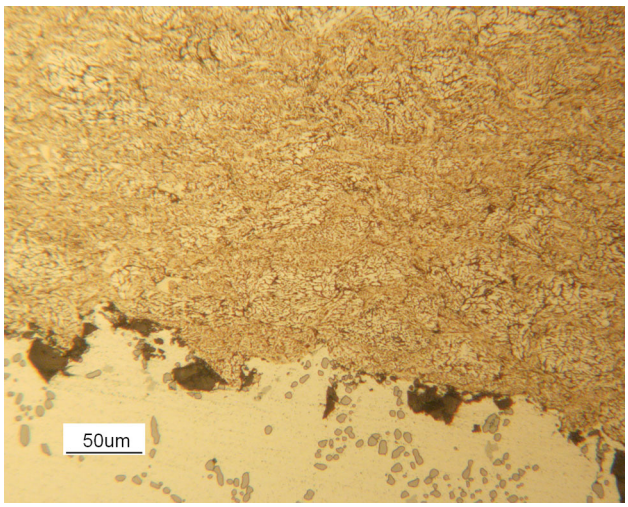

Fig. 9 Cross-sectional image of interface in vicinity of the fracture surface

underestimated. The three specimens with the same surface finish as the base material exhibited decrease in fatigue limit by 10 MPa with respect to the polished specimens. Hence, we can conclude that increase in the fatigue limit in case of the base material set would not exceed 10 MPa. This would mean that fatigue strength of the coating reaches 85% of the original material strength at minimum. This provides a very good starting point for fatigue performance of the coated or restored parts. Fatigue life may be further improved by applying optimal shot peening as a post-treatment or careful surface finishing. Rupture always occurred in the middle of the specimen exhibiting no significant delamination of the coating. The observation did not reveal any crack propagation marks in the coating and substrate. Figure 8 displays most of the fracture surface with clear distinction of peripheral coating and substrate (a), detail of the coating (b), and detail of the interface between coating and substrate (c). There are two few millimeters long and very localized cracks observed at the interface in Fig. 8(c). This may indicate delamination of the coating from substrate, which can act as fatigue crack initiation point even though surrounding does not show any evidence of it. To see whether crack progresses along the interface, cross-sectional cuts were observed by optical microscope. No coating delamination from the substrate was detected, and the whole interface appears as displayed in Fig. 9, which was taken just below the fracture surface (black spots at the interface are alumina particles from grit blasting). Embedded alumina at the interface may act as stress concentration resulting in local delamination and subsequently in fatigue crack propagation. However, the influence of surface finishing on fatigue limit described above suggests that crack was originated from free surface by

cyclic slip mechanism. For this reason, it can be concluded that cracks in Fig. 8(c) do not play major role in fatigue damage mechanism. Due to brittle nature of the coating, the crack propagates through the coating very quickly leaving no typical striation marks. Once it reaches substrate, the final fracture occurs because the load could not be sustained anymore. Fatigue testing clearly demonstrated that coating's performance is nearly as good as the original base material under cyclic loading. This represents a great step toward successful restoration of loaded components.

Conclusion

High process gas pressure and temperatures were used to deposit A357 aluminum alloy on the same material substrate. Mechanical properties of the coating were studied through series of tests and following conclusions can be made:

- Bond strength about 45 MPa (compare to Ref 36) was measured for coatings deposited on smooth surface implying that metallurgical bonding might be created in some parts of the interface. Surface state introduced by shot peening does not contribute to better bonding, and residual stress in substrate resulting from shot peening does not influence adhesion of the coating, which is about 45 MPa (same as value obtained on smooth substrate surface preparation). If substrate is grit-blasted prior coating, bond strength further increases to values above 70 MPa (failure in glue). Adhesion test also demonstrated that increase in spray temperature has positive effect on bond strength.
- Cohesion strength increases with increasing spray temperature, and it is higher than already published results (Ref 36).
- Increase in deposition temperature from 450 °C to 550 °C does not alter residual stress in the coatings, which are in both cases relatively small, compressive and equibiaxial.
- Tensile properties are significantly improved after HT, which includes solution annealing and aging. Coating's strength reaches strength of the cast A357-T61 and by nature brittle coating gain elongation exceeding 5%, which is more than value of measured on A357-T61.
- Fatigue limit of coated specimens subjected to axial push–pull test reaches 94% of the limit obtained on bulk A357-T61. Moreover, no coating's delamination was observed after the testing.

This study shows that after careful choice of process parameters and surface finish, the overall performance of cold spray A357 coatings supports feasibility of cold spray application for structural repairs, where mechanical behavior is primary requirement. In particular, it is worth noting that the fatigue tests showed that cold spray technology can be used even for the parts subjected to cyclic loads: further tests are already planned to confirm the present results. Tensile test revealed that cold spray is a suitable technology also for additive manufacturing of A357 aluminum alloy, especially, when solution heat treatment and aging is used.

Acknowledgments The research leading to these results has received funding from the European Union Seventh Framework Programme (FP7/2007-2013) under Grant Agreement No ACS3-GA-2013-605207-CORSAIR. We would like thank Peenservice srl (Bologna, Italy) for performing the shot peening treatment and group of P. Poza (URJC, Madrid, Spain) for providing us with micrographs displayed in Fig. 1.

References

1. The Welding Institute Website (2107). www.theweldinginstitute.com. Accessed 13 April 2017
2. CORSAIR (2016). www.corsair-project.eu. Accessed 13 April 2017
3. V.K. Champagne, *The Cold Spray Materials Deposition Process: Fundamentals and Applications*, 1st ed., Woodhead Publishing, Cambridge, 2007, p. 376
4. C.M. Kay and J. Karthikeyan, *High Pressure Cold Spray Principles and Applications*, 1st ed., ASM International, Materials Park, 2016, p. 300
5. J. Villafuerte, *Modern Cold Spray: Materials, Process, and Applications*, 1st ed., Springer, Berlin, 2015, p. 429
6. J. Vlcek, L. Gimeno, H. Huber, and E. Lugscheider, A Systematic Approach to Material Eligibility for the Cold-Spray Process, *J. Therm. Spray Technol.*, 2005, **14**(1), p. 125-133
7. G. Bae, Y. Xiong, S. Kumar, K. Kang, and C. Lee, General Aspects of Interface Bonding in Kinetic Sprayed Coatings, *Acta Mater.*, 2008, **56**(17), p. 4858-4868
8. A357.0–T62. www.matweb.com. Accessed 13 April 2017
9. N.D. Alexopoulos and A. Stylianos, Impact Mechanical Behaviour of Al–7Si–Mg (A357) Cast Aluminum Alloy. The Effect of Artificial Aging, *Mater. Sci. Eng.*, 2011, **528**(16–20), p. 6303-6312
10. J.R. Davis, *Aluminum and Aluminum. Alloys Alloying: Understanding the Basics*, 1st ed., ASM International, Materials Park, 2001, p. 647
11. T.J. Eden and D.E. Wolfe, Cold Spray Applications in the Defense Industry, *J High Pressure Cold Spray: Principles and Applications*, 1st ed., C.M. Kay and J. Karthikeya, Ed., ASM International, Materials Park, 2016, p. 227-251
12. H. Assadi, T. Schmidt, H. Richter, J.O. Kliemann, K. Binder, F. Gärtner, T. Klassen, and H. Kreye, On Parameter Selection in Cold Spraying, *J. Therm. Spray Technol.*, 2011, **20**(6), p. 1161-1176
13. T. Schmidt, F. Gärtner, and H. Kreye, New Developments in Cold Spray Based on Higher Gas and Particle Temperatures, *J. Therm. Spray Technol.*, 2006, **15**(4), p. 488-494
14. M.M. Sharma, T.J. Eden, and B.T. Golesich, Effect of Surface Preparation on the Microstructure, Adhesion, and Tensile Properties of Cold-Sprayed Aluminum Coatings on AA2024 Substrates, *J. Therm. Spray Technol.*, 2015, **24**(3), p. 410-422

15. R.G. Maev, V. Leshchynsky, E. Strumban, D. Dzhurinskiy, and E. Maeva, Influence of Grit Blasting on the Interface Roughness and Adhesion Strength of Cold Sprayed Copper Coatings, in *Proceedings of the International Thermal Spray Conference on Thermal Spray 2015*, ed by A. McDonald, A. Agarwal, G. Bolelli, Y. C. Lau, F. L. Toma, E. Turunen, C. Widener. 11–14 May 2015 (ASM International, Long Beach, California, USA, 2015), pp. 493–497
16. R. Ghelichi, D. MacDonald, S. Bagherifard, H. Jahed, M. Guagliano, and B. Jodoin, Microstructure and Fatigue Behavior of Cold Spray Coated Al5052, *Acta Mater.*, 2012, **60**(19), p. 6555-6561
17. A. Moridi, S.M. Hassani-Gangaraj, S. Vezzú, L. Trško, and M. Guagliano, Fatigue Behavior of Cold Spray Coatings: the Effect of Conventional and Severe Shot Peening as Pre-/Post-Treatment, *Surf. Coat. Technol.*, 2015, **283**(15), p. 247-254
18. A.C. Hall, D.J. Cook, R.A. Neiser, T.J. Roemer, and D.A. Hirschfeld, The Effect of a Simple Annealing Heat Treatment on the Mechanical Properties of Cold-Sprayed Aluminum, *J. Therm. Spray Technol.*, 2006, **15**(2), p. 233-238
19. M.R. Rokni, C.A. Widener, V.K. Champagne, and S.R. Nutt, The Effects of Heat Treatment on 7075 Al Cold Spray Deposits, *Surf. Coat. Technol.*, 2017, **310**, p. 278-285
20. O.S. Es-Said, D. Lee, W.D. Pfost, D.L. Thompson, M. Patterson, J. Foyos, and R. Marloth, Alternative Heat Treatments for A357-T6 Aluminium Alloy, *Eng. Fail. Anal.*, 2002, **9**(1), p. 99-107
21. Standard Test Method for Adhesion or Cohesion Strength of Thermal Spray Coatings", C633, Annual Book of ASTM Standards, ASTM, 2013, p. 8
22. Size Classification and Characteristics of Ceramic Shot for Peening, J1830_201310, (SAE International, 1987), p. 3
23. S. Baiker, *Shot Peening: A Dynamic Application and Its Future*, 4th ed., MFN - Metal Finishing News, 2006, p. 18
24. G.P. Zanon and S. Vezzu, Method for Repairing an Aluminium Alloy Component, WO Patent App. PCT/IB2012/051,434, 28 Sept 2012
25. F. Gärtner, T. Schmidt, and H. Kreye, in TCT Test, Institute of materials technology (HSU, Hamburg). www.hsu-hh.de. Accessed 13 April 2017
26. Standard Test Methods for Tension Testing of Metallic Materials, E8/E8M, Annual Book of ASTM Standards, ASTM, 2013, p. 30
27. W. Dixon and F. Massey, *Introduction to Statistical Analysis*, 3rd ed., McGraw-Hill, New York City, 1969, p. 488
28. T. Hussain, D.G. McCartney, P.H. Shipway, and D. Zhang, Bonding Mechanisms in Cold Spraying: The Contributions of Metallurgical and Mechanical Components, *J. Therm. Spray Technol.*, 2009, **18**(3), p. 364-379
29. H. Assadi, F. Gärtner, T. Stoltenhoff, and H. Kreye, Bonding Mechanism in Cold Gas Spraying, *Acta Mater.*, 2003, **51**(15), p. 4379-4394
30. K. Spencer, V. Luzin, N. Matthews, and M.X. Zhang, Residual Stresses in Cold Spray Al Coatings: The Effect of Alloying and of Process Parameters, *Surf. Coat. Technol.*, 2012, **206**, p. 4249-4255
31. G. Shayegan, H. Mahmoudi, R. Ghelichi, J. Villafuerte, J. Wang, M. Guagliano, and H. Jahed, Residual Stress Induced by Cold Spray Coating of Magnesium AZ31B Extrusion, *Mater. Des.*, 2014, **60**, p. 72-84
32. K. Ogawa and D. Seo, Repair of Turbine Blades Using Cold Spray Technique, *Advances in Gas Turbine Technology*, 1st ed., E. Benini, Ed., InTech, Croatia, 2011, p. 499-526
33. Q. Wang, D. Qiu, Y. Xiong, N. Birbilis, and M.X. Zhang, High Resolution Microstructure Characterization of the Interface Between Cold Sprayed Al Coating and Mg Alloy Substrate, *Appl. Surf. Sci.*, 2014, **289**, p. 366-369
34. ASM International, *ASM Handbook Volume 2 Properties and Selection: Nonferrous Alloys and Special-Purpose Materials*, ASM International, Materials Park, 1990
35. V. Luzin, K. Spencer, and M.-X. Zhang, Residual Stress and Thermo-Mechanical Properties Of Cold Spray Metal Coatings, *Acta Mater.*, 2011, **59**(3), p. 1259-1270
36. S. Rech, A. Trentin, S. Vezzù, and G.P. Zanon, High Thickness A-357 Aluminium Alloys Coatings Deposited by Cold Spray for the Repair of Aeronautic Components, in *International Thermal Spray Conference (poster), Hamburg, 2011*